A Simple Description of Turn-Induced Transverse Field Dispersion in Microfluidic Channels for System-Level Design

R. Magargle*, J.F. Hoburg** and T. Mukherjee***

Carnegie Mellon University, Pittsburgh, PA 15213, USA
*magargle@cmu.edu, **hoburg@ece.cmu.edu, ***tamal@ece.cmu.edu

ABSTRACT

This paper shows a simple analytical model for turn-induced dispersion that captures an essential aspect of the transition field from uniform to circumferential that has been ignored in prior simple descriptions [1,2,3,4]. The model applies directly to the high Peclet number regime, which is relevant to DNA separations [5], but identifies a new dispersion mechanism that is present in all regimes. The results of this model are compared with numerical simulation and experimental results. Comparisons to previous models [2,3,4] show significant differences, about a factor of 4, in the expected variance for high Peclet complementary turns.

Keywords: turn, complementary, dispersion, electrokinetic, design

1 INTRODUCTION

In high Peclet regimes, previous models [1,2,3,4] assume that a band is skewed linearly after a single turn. For these systems, skew is defined as the amount the inside of the band leads the outside after traveling through a bend and the Peclet number is defined by $Pe_w=Uw/D$, where U is the average band velocity, w is the channel width, and D is the diffusion coefficient. This linear skew assumption is used to determine the variance due to a single turn, $\sigma^2_{turn}=(skew)^2/12$, with $skew=(2\theta w)$, where θ is the angle of the curve and w is the channel width. The linear skew approximations, while nearly but not exactly correct for a single turn, ignore two separate effects that are each significant for complementary turns:

1) Even an "abrupt" electric field model that ignores the Laplacian transition between straight and curved sections yields significant dispersion after complementary turns, and
2) The Laplacian transition field significantly increases dispersion (by about a factor of 4 for the results shown here) over what is predicted by the abrupt transition model.

This paper shows accurate field models and dispersion descriptions that are suitable for integration into automated software synthesis design engines. The paper first describes the abrupt field model, which assumes that the field structure is discontinuous at the straight-curve interface. Then a correction that accounts for the Laplacian transition field between straight and curved sections is described, and it is shown to have a significant impact on the predicted band dispersion compared to the abrupt field structure, and the linear skew predictions. Because of the difference in results for complementary turns, the full description is suitable for implementation into an accurate automated software synthesis design engine when diffusion effects are relatively small. Finally, comparisons between the Laplacian full-field model, Femlab PDE solutions and experiment are shown.

2 ELECTRIC FIELD MODELS

Currently published analytical electrokinetic dispersion models ignore significant electrostatic field components in the transition region from a straight to a curved channel [1,2,3,4]. These missing field components can be accounted for by adding Laplacian correction field solutions to the straight and curved channel abrupt field equations. The Laplacian correction field components significantly impact the dispersion of particles traveling through a bend, as will be seen in Section 3. The missing field components are apparent when a PDE solution to the electrostatic field is compared to the abrupt field transition solution, as seen in Figure 1.

The effect of the turn is seen well before the actual straight-curve interface, as the equipotential lines begin to bend even in the straight section. This effect is even more pronounced as the ratio of width to center radius, w/r_c, increases.

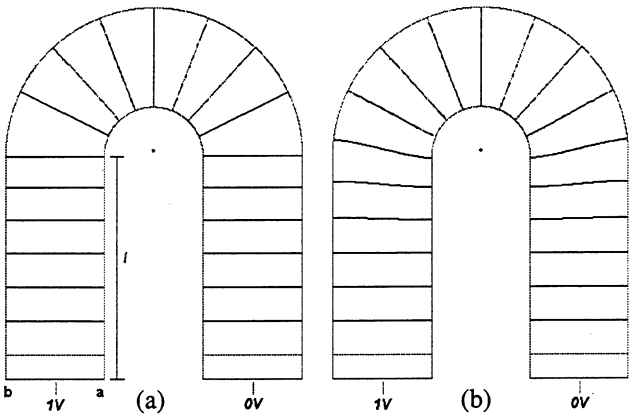

Figure 1 – (a) Abrupt transition field equipotential lines (b) Laplacian electrostatic transition field equipotential lines.

2.1 Abrupt Field Model

In the abrupt transition model that is represented by Figure 1(a), the field in the straight sections has a constant value, while the field in the curved section is circumferentially directed, with a magnitude that decreases as *1/r*. The fields in each section are determined by requiring continuity of total current across the channel width and by setting the total line integral of electric field equal to the applied voltage:

$$E_y^{straight} = \frac{V_{app}\ln(b/a)}{2l\ln(b/a)+w\pi} \tag{1}$$

$$E_\phi^{curve} = \frac{wV_{app}}{r(2l\ln(b/a)+w\pi)} \tag{2}$$

Since E_ϕ^{curve} varies with radius, these fields are discontinuous along the lines where straight and curved sections meet. For this reason, an accurate description of the field structure requires a correction that corresponds to the smooth transition that is apparent in Figure 1(b).

2.2 Laplacian Field Model

Expressing the potential in each section as the sum of the abrupt field and a series of Fourier components, each of which satisfies Laplace's equation, and requiring continuity of the resulting field components, the fields are expressed as follows:

$$E_r^{curve} = \sum_n \frac{C_n}{r}\exp\left(\frac{-n\pi\phi}{\ln(b/a)}\right)\sin\left(n\pi\frac{\ln(r/a)}{\ln(b/a)}\right)$$

$$E_\phi^{curve} = \frac{V_{co}}{r} + \sum_n \frac{C_n}{r}\exp\left(\frac{-n\pi\phi}{\ln(b/a)}\right)\cos\left(n\pi\frac{\ln(r/a)}{\ln(b/a)}\right)$$

$$E_x^{straight} = \sum_n D_n \frac{n\pi}{w}\sin\left(\frac{n\pi x}{w}\right)\exp\left(\frac{n\pi y}{w}\right)$$

$$E_y^{straight} = E_{so} - \sum_n D_n \frac{n\pi}{w}\cos\left(\frac{n\pi x}{w}\right)\exp\left(\frac{n\pi y}{w}\right)$$

(3)

where V_{co} and E_{so} are determined from the abrupt fields in equations (1) and (2), and C_n and D_n are determined by matching field components for a finite number of terms in the Fourier Series. If only a single term (the first order correction) is used, C_1 and D_1 are

$$C_1 = \frac{-g_1}{f_1+h_1},\quad D_1 = \frac{-f_1 g_1}{\pi(f_1+h_1)} \tag{4}$$

where f_1, g_1, and h_1 are

$$f_1 = \int_0^w \frac{2}{x+a}\sin\left(\pi\frac{\ln(x/a+1)}{\ln(b/a)}\right)\sin\left(\frac{\pi x}{w}\right)dx \tag{5}$$

$$g_1 = \int_0^w 2E_{so}\left(\frac{b-a}{(x+a)\ln(b/.a)}-1\right)\cos\left(\frac{\pi x}{w}\right)dx \tag{6}$$

$$h_1 = \int_0^w \frac{2}{x+a}\cos\left(\pi\frac{\ln(x/a+1)}{\ln(b/a)}\right)\cos\left(\frac{\pi x}{w}\right)dx \tag{7}$$

Even using only a single term of the series (the first order correction), excellent agreement with PDE solvers such as the Ansoft Maxwell finite element program is obtained for w/r_c up to 1.0.

A comparison of the abrupt and Laplacian field descriptions is shown in Figures 2 and 3.

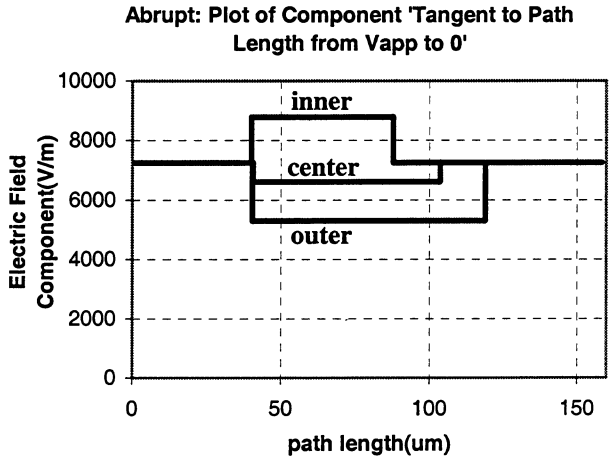

Figure 2 – Abrupt field circumferential component

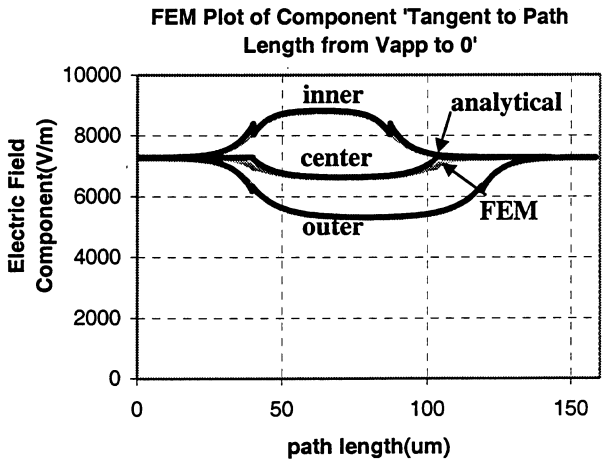

Figure 3 – Full Laplacian correction field circumferential component compared with FEM solution

The Laplacian Fourier series solution in Figure 3 is almost indistinguishable from the FEM solution, and their agreement further increases as w/r_c decreases.

3 FIELD INDUCED DISPERSION

In this section, the effects of field induced dispersion due to abrupt and Laplacian fields through complementary turns are shown. This difference is shown in Figure 4 for a band as it travels through three sets of complementary turns. The simulations follow trajectories of particles along the front and back edges of a band, and do not include the effects of diffusion (infinite Peclet number). This regime applies, for example, to DNA separation [5]. The results displayed are obtained from infinite Peclet "particle simulations" created in Matlab.

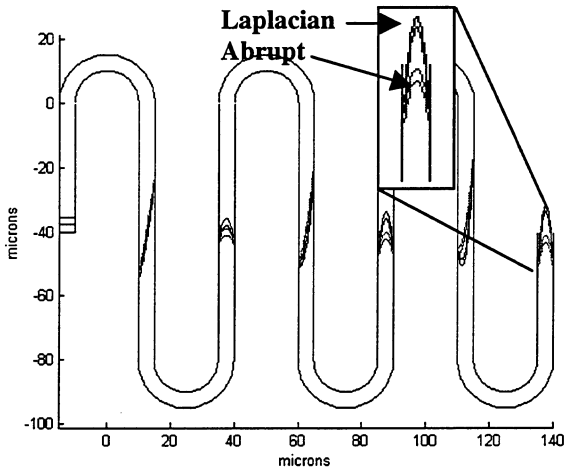

Figure 4 - High Peclet band dispersion for $w/r_c = 0.4$ (band moves from left to right).

Particle simulations of this kind show that the Laplacian field difference is small after a single turn; however, both Laplacian and abrupt descriptions deviate from the linear skew approximations [1,2,3,4], especially after one or more sets of complementary turns, where the linear skew incorrectly predicts zero turn-induced variance.

The Laplacian field produces approximately 4 times the dispersion of the abrupt field for a single pair of complementary turns, to within ~3%, for a w/r_c range of 0.1 to 0.4. Similarly, by comparing the dispersion of the two descriptions after an arbitrary number of sets of complementary turns, it can be seen that the difference between the two is constant after each set of turns, ~4 for w/r_c=0.4. For both the abrupt and Laplacian descriptions in the high Peclet regime, the dependence of variance upon the number of sets of complementary turns is quadratic.

Figure 5 shows the results of a band traveling through six sets of complementary turns. For both the abrupt and Laplacian fields, when the band travels through multiple sets of complementary turns in the high Peclet regime, as in Figure 4, it experiences a quadratic variance in growth with the number of sets of complementary turns.

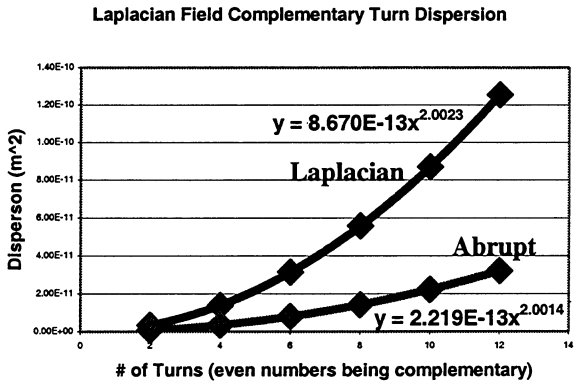

Figure 5 – Growth of band variance with number of complementary turns, up to 6 sets, in abrupt and Laplacian fields for w/r_c=0.4

3.1 Femlab Simulation Comparisons

To verify the particle simulation results, Femlab was used as a PDE solver to compare to the particle simulations and relevant experimental results, such as those in [3]. Femlab is unique in that it allows the subdomains of the problem to be specified independently. This allows for use of the abrupt fields, by specifying the equations from Section 2.1 and associating them with the appropriate straight or curved section. To simulate the Laplacian fields, the PDE solver is used to compute the full field solution.

Figure 6 shows the Femlab results for one set of complementary turns with w/r_c =0.4.

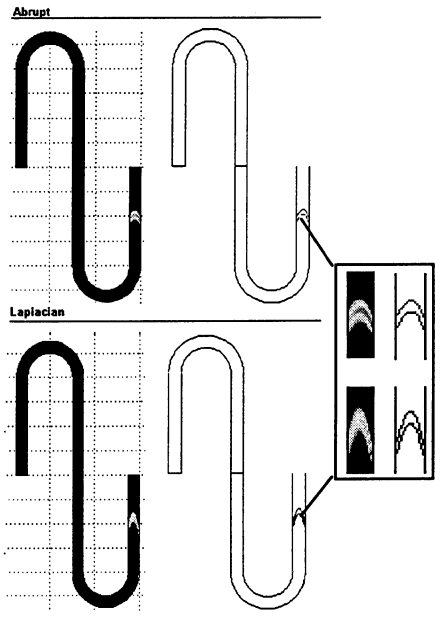

Figure 6 - Femlab simulations on the left compared to particle simulations on the right for $w/r_c = 0.4$. Results from the abrupt field model are on top and from the Laplacian transition field are on bottom.

To compare Femlab's results with an experiment that involves significant diffusion, as apposed to the high Peclet simulations above, a low Peclet simulation was run to coincide with the experimental setup in [3]. The results of this simulation are seen in Figure 7 with Pe_w=138.

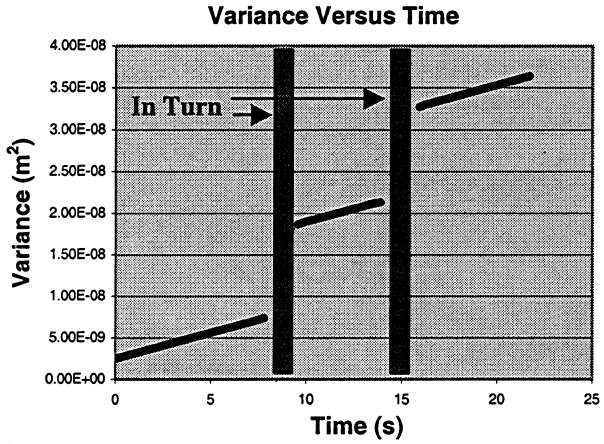

Figure 7 – Band variance through geometry in [3] with Pe_w=138.

Figure 7 is similar to the plot in [3]. The variance of the band as it travels through the channel is plotted versus the time traveled. As in [3], the slope of this plot should be twice the diffusion, since the variance due to diffusion alone is $\sigma^2_D=2Dt$. The jump in variance after the vertical bar representing the turn is the additional variance due to the curve, σ^2_{geo}. The slope of the curve in Figure 7(a) is 3.12e-10m^2/s, and the jump in variance is 1.01e-8m^2. These results are in agreement with the data in [3] when the variance data in [3] is adjusted to take into consideration the mean channel width, as discussed in [2,4].

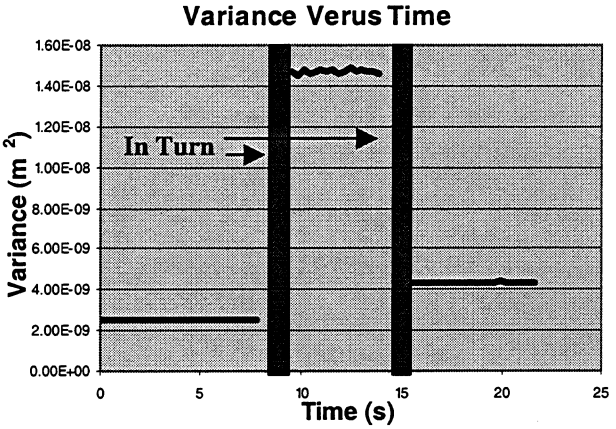

Figure 8 - Band variance through geometry in [3] with a Pe_w=16000.

Figure 8 shows a high Peclet version of the simulation described by Figure 7. This high Peclet Femlab simulation demonstrates the same turn-induced dispersion behavior as the particle simulations (infinite Peclet) described in previous sections.

Figure 8 also shows that in contrast with the linear skew description, a net variance remains with a value even larger than that predicted by the transition field model, due to diffusion even in this regime, and much larger than that predicted by an abrupt field model.

4 CONCLUSION

In this paper, simple expressions that accurately describe the Laplacian transition electrostatic field in a curved microchannel are shown. It is also shown that significant differences exist between the predicted band dispersion using abrupt and Laplacian electrostatic fields, and that both descriptions exhibit quadratic growth through multiple sets of complementary turns. High Peclet Femlab simulations are compared with high Peclet particle simulations using abrupt and Laplacian fields, and low Peclet Femlab simulations are compared with experiments in [3], all with good agreement.

ACKNOWLEDGEMENTS

This research effort is sponsored by the Defense Advanced Research Projects Agency under the Air Force Research Laboratory, Air Force Material Command, USAF, under grant number F30602-01-2-0587.

REFERENCES

[1] Griffiths, S.K., Nilson, R. H., Vol. 73, Analytical Chemistry 2001, pp. 272-278.

[2] Molho, J.I., Herr, A.E., Mosier, B.P., Santiago, J.G., Kenny, T.W., et.al., Vol. 73, Analytical Chemistry 2001, pp. 1350-1360.

[3] Culbertson, C.T., Jacobson, S.C., Ramsey, M.I., Vol. 70, Anal. Chem. 1998, pp. 3781-3789.

[4] Griffiths, S. K., Nilson, R. H., Vol. 72, Analytical Chemistry 2000, pp. 5473-5482.

[5] Paegel, B.M., Hutt, L.D., Simpson, P.C., Mathies, R.A., Vol. 72 Analytical Chemistry 2000, pp.3030-3037.